Supporting information

Defect-assisted surface modification in g-C_3N_4@WC heterostructure for tetracycline degradation: DFT calculation, degradation pathways, and nematode-based ecological assessment

Athibala Mariappan[a], Govindhan Thiruppathi[b], Govindan Bharath[c], Palanisamy Sundararaj[b], Ranjith Kumar Dharman[a], Tae Hwan Oh[a*]*

[a] *School of Chemical Engineering, Yeungnam University, Gyeongsan, 38541, South Korea*

[b] *Department of Zoology, Bharathiar University, Coimbatore, Tamil Nadu 641046, India*

[c] *Department of Physics and Nanotechnology, SRM Institute of Science and Technology, Kattankulathur, Chennai-603203, Tamil Nadu, India*

Corresponding author mail id:

T.H.O (taehwanoh@ynu.ac.kr)

R.K.D (amaranjith@gmail.com)

Table of contents

Characterization techniques

The crystal structures of the obtained samples were analyzed using X-ray diffraction (XRD, Xpert Pro equipped with Cu Kα radiation). The morphological structures were examined using Field emission scanning microscopy (FESEM) (FE-SEM HITACHI S-4800 and transmission electron microscopy (HRTEM) (Titan G2 ChemiSTEM Cs probe). The chemical bonding information was studied using by X-ray Photoelectron Spectroscopy (XPS Thermo scientific K-α surface analysis). The optical properties of the as-prepared samples were measured by UV-vis Spectrometer (VARIAN 5000). The photoluminescence spectra were measured using (PL, LabRAM HR Evolution) and carrier life-time studies were investigated using time-resolved photoluminescence spectra (TRPL, using a fluorescence spectrometer (FL3, Horiba)). The reactive oxygen species were examined using an electron spin resonance spectrometer (ESR, Bruker, EMX plus-9.5/2.7). The photodegradation reaction pathways are explored by (LC-MS, High-resolution Liquid Chromatography Mass Spectroscopy, Thermofisher (Q Exactive vanquish)).

Ecotoxicological Assessment

All *C. elegans* strains employed for this study were obtained from the *Caenorhabditis* Genetics Center (CGC, University of Minnesota, MN). Worms were preserved on nematode growth media (NGM) agar plates and age synchronized based standardized procedures [1, 2] [3]. Further, the *in vivo* toxicity assay was executed as previously described [4] [5]. In detail, age-synchronized young adult worms (20-30 individuals/replicate) were transferred to microtiter plates carrying 1 mL of test solution containing degraded Tetracycline (**DT**) or non-degraded Tetracycline (**N-DT**) and heat-killed of *E. coli* strain OP50 (6 mg/mL). After 24 h of continuous

exposure, the worms were recorded for various assays. For acute toxicity assessment, the control and treated worms were examined for inactivity under a stereo zoom microscope. The worms were considered dead when they lost their intact body structures and pharyngeal pumping. In order to measure the reproductive rate, the worms were individually transferred to fresh NGM plates each day during their reproductive phase, and the eggs laid by each worm were allowed to develop and counted at the L4 stage. The body length (development) of the worms from the control and treated groups was measured using Optika IS view image processing software by measuring the flat surface area as described. The rhythmic contraction and relaxation of the pharynx (pharyngeal pumping) of worms were measured to assess the effect of degraded or non-degraded Tetracycline on the metabolic rate of *C. elegans*. The locomotion behavior of worms was measured by monitoring body bends. After appropriate treatment, the worms were transferred to new NGM plates and allowed to crawl freely for 5 min. Afterwards, the worms were individually shifted onto microscopic slides containing 1 mL of M9 buffer, and the reciprocating motion of bending at the mid-body of *C. elegans* was considered a body bend. The intracellular ROS levels in worms were measured using a fluorescent probe 2',7'-dichlorodihydrofluorescein diacetate (H_2DCF-DA). At indicated time points, control and treated worms were exposed to 50 µM of H_2DCF-DA for 30 mins at 20°C in the dark. Subsequently, the worms were washed thrice with M9 buffer, immobilized with 25 mM sodium azide, and mounted on 3% agar-padded microscopic slides. Photomicrographs were captured using an upright fluorescence microscope (CX43, Olympus, Japan), and ROS levels were measured by quantifying the intensity of DCF signals with ImageJ freeware (NIH, Bethesda, MD). To examine the effect of degraded and non-degraded Tetracycline on the expression of stress-responsive genes (*sod-3*, *gst-4*, and *ctl-1,2,3*) in *C. elegans*, transcriptional reporter strains *viz*.,

CF1553 (*sod-3::GFP*), CL2166 (*gst-4::GFP*), and GA800 (*ctl-1,2,3::GFP*) were used. The worms (~20 worms/experiment) were exposed to degraded or non-degraded Tetracycline and imaged using a fluorescence microscope as described above. Finally, the GFP signal was quantified using ImageJ. All experiments were performed at least three times with appropriate replicates under similar conditions, and the obtained datas were analyzed using one-way analysis of variance (ANOVA) followed by Bonferroni's post hoc test. The level of $p<0.05$ was considered significant.

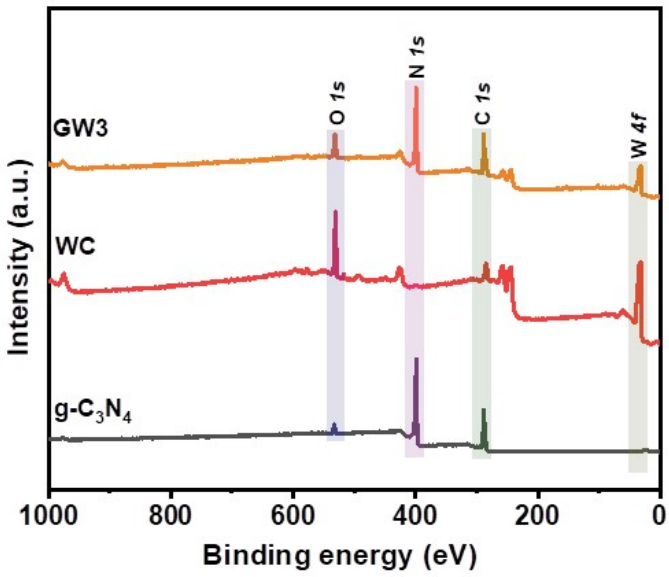

Fig. S1. XPS survey scan spectrum of gC_3N_4, WC, and GW3 catalysts.

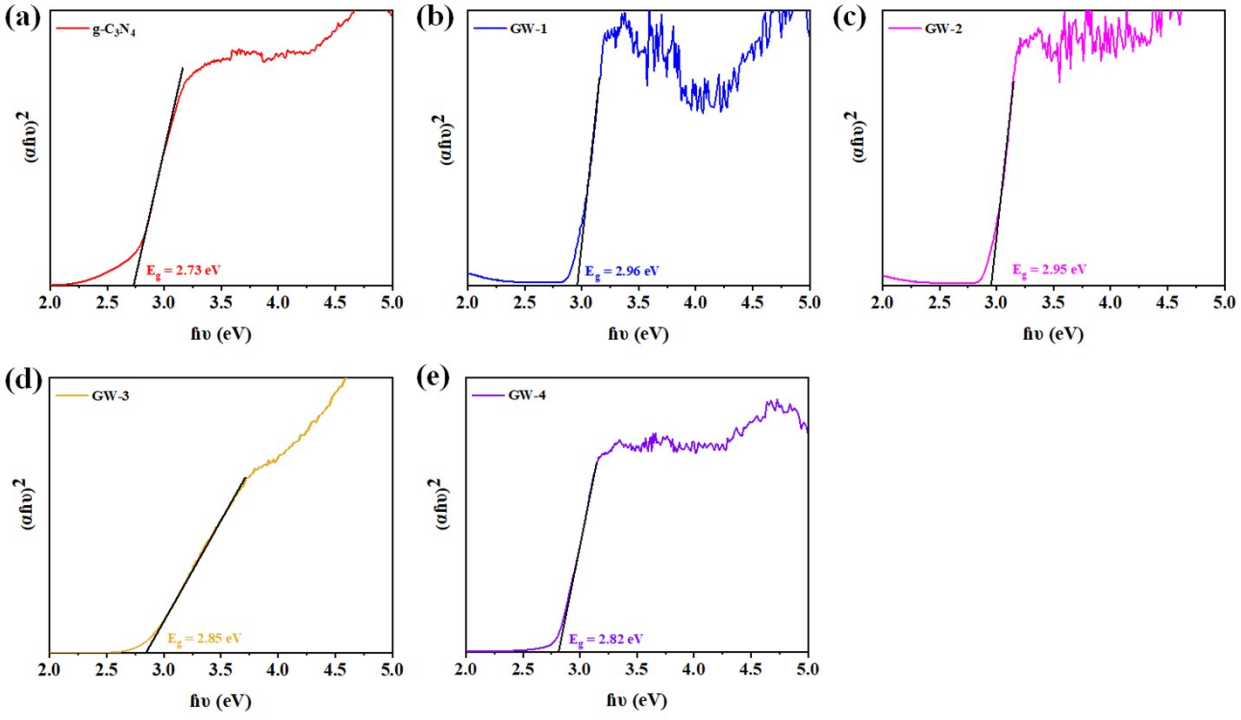

Fig. S2. The Tauc plot of the different photocatalysts.

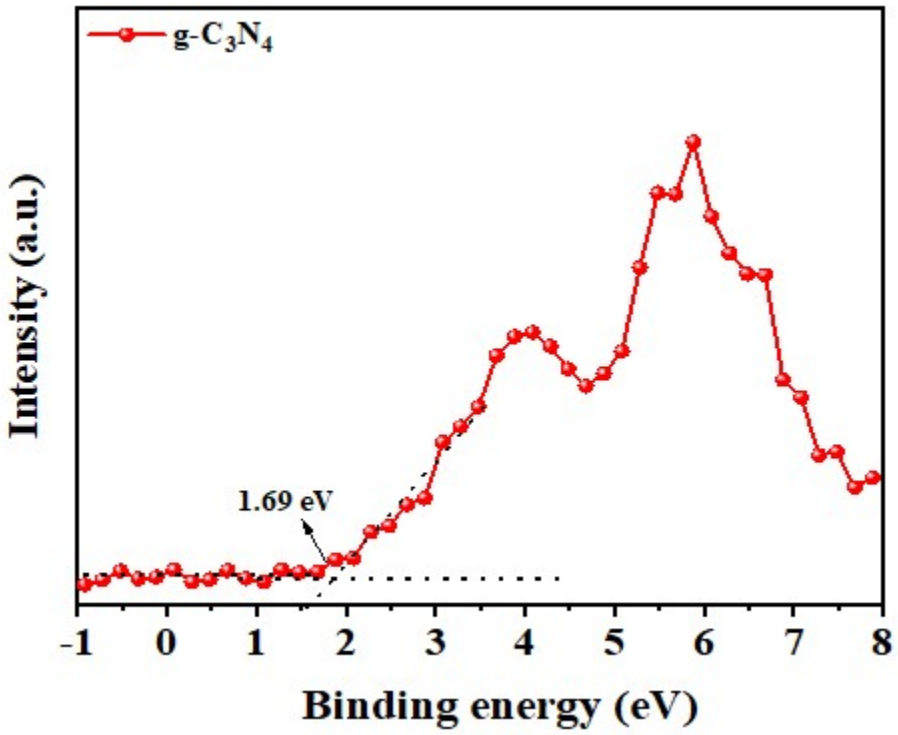

Fig. S3. Valance band spectra of g-C_3N_4 photocatalyst.

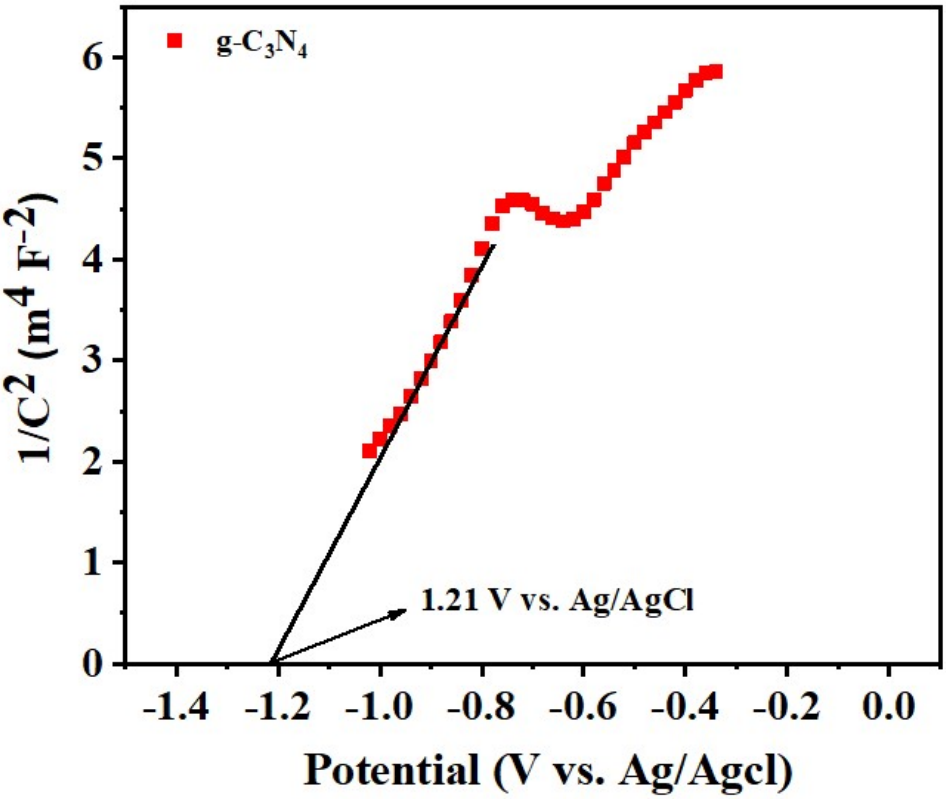

Fig. S4. Mott-Schottky plot of g-C_3N_4.

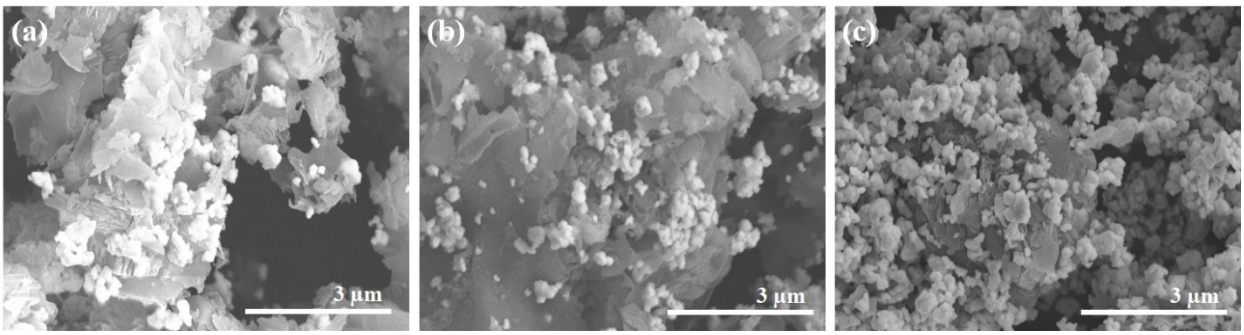

Fig. S5. FESEM images of (a), GW1, (b) GW2 and (c) GW4.

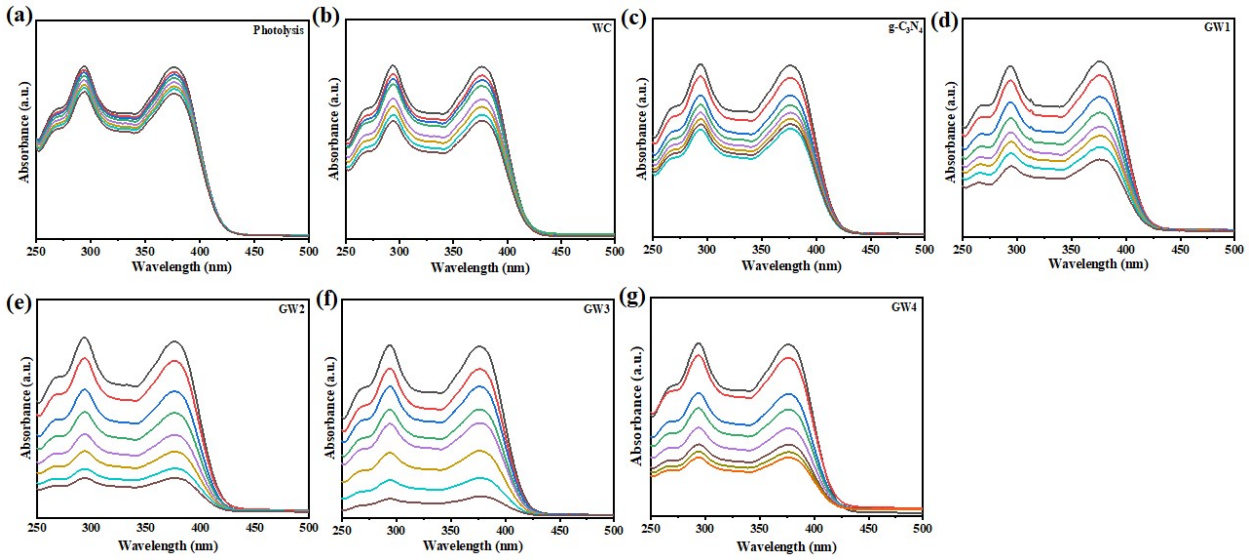

Fig. S6. UV-Visible spectra of different photocatalysts.

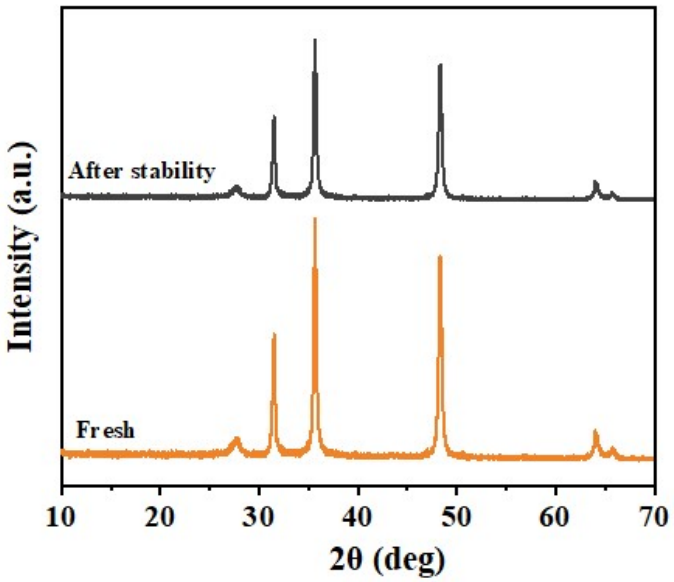

Fig. S7. XRD pattern of fresh and after stability GW3 catalyst.

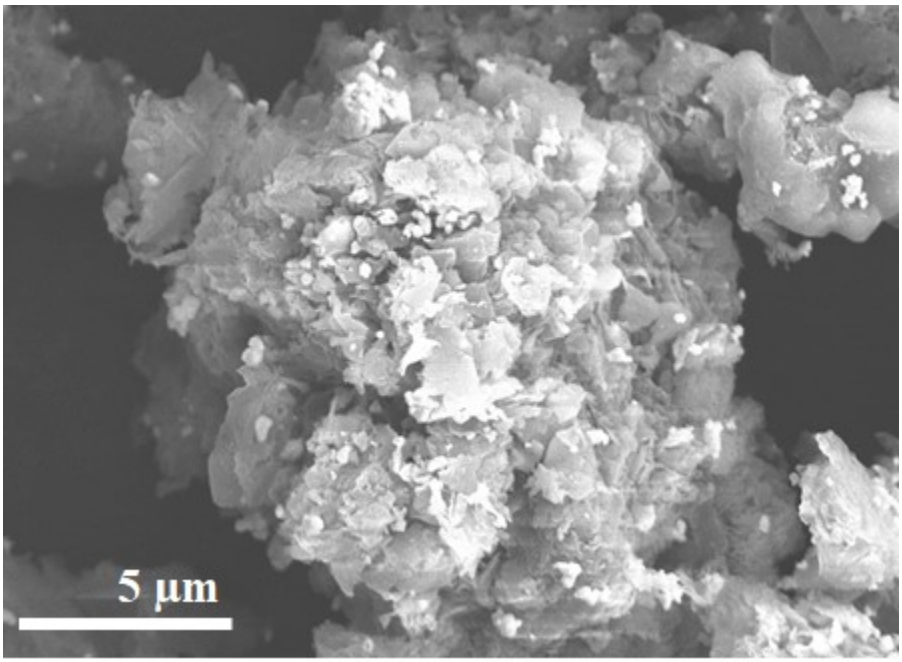

Fig. S8. FESEM image of GW3 (after stability).

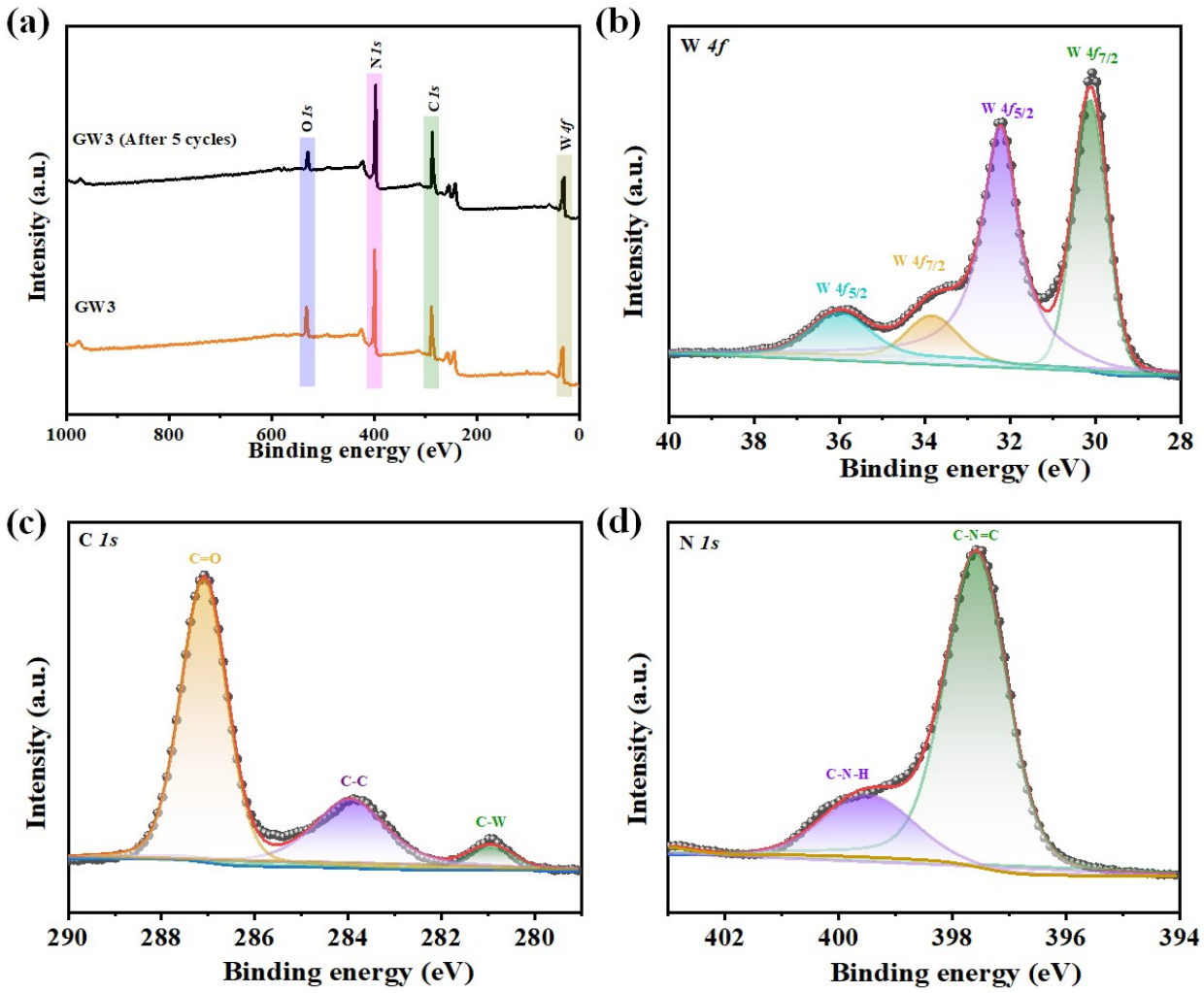

Fig. S9. XPS survey spectra of GW3 and GW3 (after stability), High-resolution W *4f* (b), C *1s*, and (d) N *1s* spectra of GW3 (after stability).

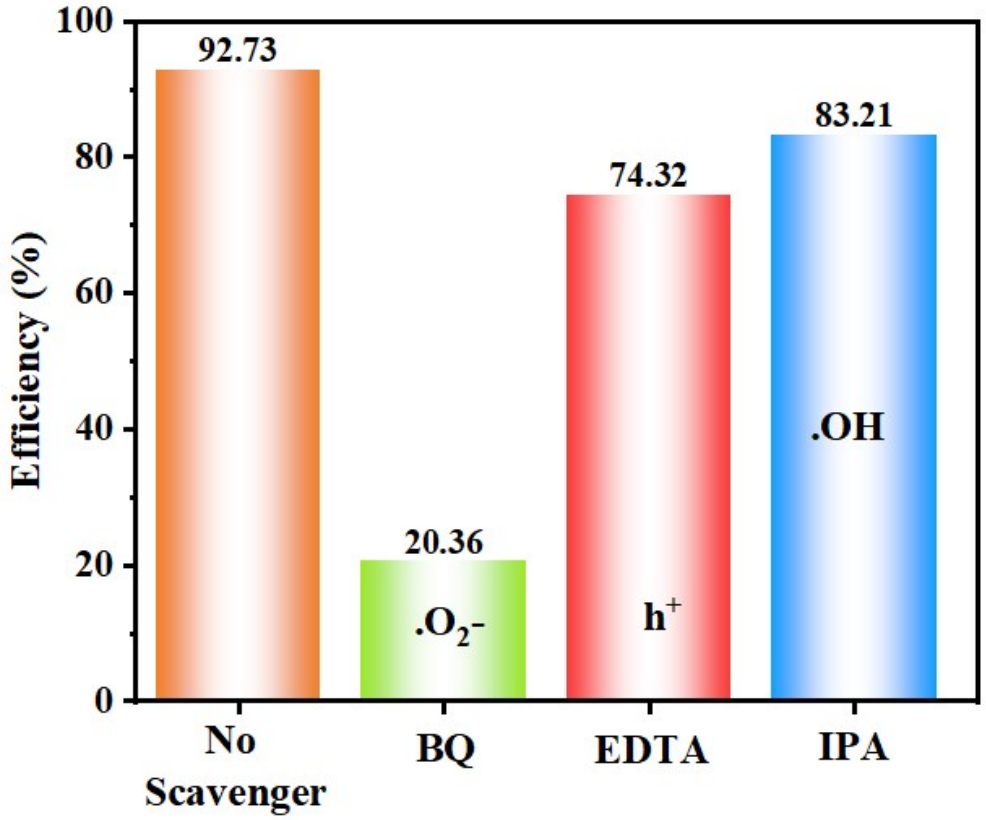

Fig. S10. Trapping experiment using different scavengers for GW3 photocatalysts.

Table S1. Summary of previously reported gCN based heterostructure towards photodegradation of antibiotics

Catalysts	Pollutant	Light source	Degradation efficiency (%)	Total time (min)	Ref
K,P co- doped gCN/$CoFe_2O_4$	Tetracycline	500 W halogen lamp	85	60	[6]
α-MnO_2/HT-gCN	Ciprofloxacin	300 W Xenon lamp	89.2	90	[7]
BiOI/$BiVO_4$/g-C_3N_4	Levofloxacin	65 W energy saving lamp	89.01	120	[8]
Bi_2WO_6/Fe_3O_4/g-C_3N_4	Levofloxacin	150 W LED light	84.5	50	[9]
La-ZnO/gCN	Tetracycline	1000 W halogen lamp	84	80	[10]
CZ@T-GCN	Amoxicillin	300 W Xenon lamp	84	120	[11]
$ZnCr_2O_4$/g-C_3N_4	Ciprofloxacin	Halogen lamp	74.36	120	[12]
3D gCN/hydrogel	Tetracycline	250 W mercury lamp	86	40	[13]
Ni-doped α-Fe_2O_3/g-C_3N_4	Ciprofloxacin	Solar light (~660 Wm^{-2})	82	120	[14]

gCN/Ti_3C_2 MXene	Cefixime	45 W fluorescence lamp	64.69	105	[15]
$ZnCo_2O_4$/g-C_3N_4	Ciprofloxacin	Halogen lamp	80	120	[16]
50-Zn/gCN	Cefazolin	300 W solar lamp	78	120	[17]
Bi_5O_7I/gCN/biochar	Doxycycline	500 W halogen lamp	90.21	90	[18]
$Pr_2Sn_2O_7$/P@g-C_3N_4/SnS_2	Tetracycline	50 W halogen lamp	89.48	60	[19]
Ag/g-C_3N_4	Ciprofloxacin	5 W visible light	84	120	[20]
Ag/gC_3N_4/ZnO	Cefalexin & Amoxicillin	300 W solar lamp	71.74 & 41.36	180	[21]
WO_3/gCN/MWCNT	Tetracycline	500 W halogen lamp	79.54	120	[22]
g-C_3N_4@WC	**Tetracycline**	**250 W xenon arc lamp**	**92.73**	**120**	**This work**

References:

[1] S. Brenner, The genetics of Caenorhabditis elegans, Genetics, 77 (1974) 71-94.

[2] A. Mohankumar, G. Shanmugam, D. Kalaiselvi, C. Levenson, S. Nivitha, G. Thiruppathi, P. Sundararaj, East Indian sandalwood (Santalum album L.) oil confers neuroprotection and geroprotection in Caenorhabditis elegans via activating SKN-1/Nrf2 signaling pathway, RSC advances, 8 (2018) 33753-33774.

[3] T. Stiernagle, Maintenance of Caenorhabditis elegans, WormBook, (2021) 3-4.

[4] A. Mohankumar, G. Devagi, G. Shanmugam, S. Nivitha, P. Sundararaj, F. Dallemer, P. Kalaivani, R. Prabhakaran, Organoruthenium (II) complexes attenuate stress in Caenorhabditis elegans through regulating antioxidant machinery, European Journal of Medicinal Chemistry, 168 (2019) 123-133.

[5] M. Schieber, N.S. Chandel, ROS function in redox signaling and oxidative stress, Current biology, 24 (2014) R453-R462.

[6] R. Kumar, A. Sudhaik, Sonu, V.-H. Nguyen, Q. Van Le, T. Ahamad, S. Thakur, N. Kumar, C.M. Hussain, P. Singh, P. Raizada, Graphene oxide modified K, P co-doped g-C3N4 and CoFe2O4 composite for photocatalytic degradation of antibiotics, Journal of the Taiwan Institute of Chemical Engineers, 150 (2023) 105077.

[7] S.N.M. Raj, V.K. Jothi, A. Rajaram, P. Suresh, K. Murugan, A. Natarajan, Rational design of α-MnO2/HT-GCN nanocomposite for effective photocatalytic degradation of ciprofloxacin and pernicious activity, Environmental Science and Pollution Research, 30 (2023) 90689-90707.

[8] P. Zhu, D. Luo, M. Liu, M. Duan, J. Lin, X. Wu, Flower-globular BiOI/BiVO4/g-C3N4 with a dual Z-scheme heterojunction for highly efficient degradation of antibiotics under visible light, Separation and Purification Technology, 297 (2022) 121503.

[9] Z.H. Jabbar, B.H. Graimed, A.A. Okab, S.H. Ammar, A.A. Najim, A.Y. Radeef, A.G. Taher, Preparation of magnetic Fe_3O_4/g-C_3N_4 nanosheets immobilized with hierarchal Bi2WO6 for boosted photocatalytic reaction towards antibiotics in aqueous solution: S-type charge migration route, Diamond and Related Materials, 142 (2024) 110817.

[10] R.R. Chandrapal, J. Raveena, G. Bakiyaraj, S. Bharathkumar, V. Ganesh, J. Archana, M. Navaneethan, Enhancing the photocatalytic performance of g-C_3N_4 (GCN) via La–ZnO nanocomposite (Z-scheme mechanism) against toxic pharmaceutical pollutant, Journal of Materials Research, 38 (2023) 3585-3601.

[11] M. Moradi, F. Hasanvandian, A.A. Isari, F. Hayati, B. Kakavandi, S.R. Setayesh, CuO and ZnO co-anchored on g-C3N4 nanosheets as an affordable double Z-scheme nanocomposite for photocatalytic decontamination of amoxicillin, Applied Catalysis B: Environmental, 285 (2021) 119838.

[12] R.R. Chandrapal, K. Bharathi, G. Bakiyaraj, S. Bharathkumar, Y. Priyajanani, S. Manivannan, J. Archana, M. Navaneethan, Harnessing ZnCr2O4/g-C3N4 nanosheet heterojunction for enhanced photocatalytic degradation of rhodamine B and ciprofloxacin, Chemosphere, 350 (2024) 141094.

[13] A. Balakrishnan, E.S. Kunnel, R. Sasidharan, M. Chinthala, A. Kumar, 3D black g-C3N4 isotype heterojunction hydrogels as a sustainable photocatalyst for tetracycline degradation and H2O2 production, Chemical Engineering Journal, 475 (2023) 146163.

[14] C. Naga Lakshmi, M. Irfan, R. Sinha, N. Singh, Magnetically recoverable Ni-doped iron oxide/graphitic carbon nitride nanocomposites for the improved photocatalytic degradation of ciprofloxacin: Investigation of degradation pathways, Environmental Research, 242 (2024) 117812.

[15] A. Kumar, P. Majithia, P. Choudhary, I. Mabbett, M.F. Kuehnel, S. Pitchaimuthu, V. Krishnan, MXene coupled graphitic carbon nitride nanosheets based plasmonic photocatalysts for removal of pharmaceutical pollutant, Chemosphere, 308 (2022) 136297.

[16] R. Roshan Chandrapal, G. Bakiyaraj, S. Bharathkumar, V. Ganesh, J. Archana, M. Navaneethan, Novel combustion technique synthesis of ZnCo2O4 nanobeads/g-C3N4 nanosheet heterojunction photocatalyst in-effect of enhancing photocatalytic degradation for environmental remediation, Surfaces and Interfaces, 41 (2023) 103269.

[17] I.L. Ouriques Brasileiro, V.S. Madeira, A.L. Lopes-Moriyama, M.L. Rodrigues de Almeida Ramalho, Addition of g-C3N4 to ZnO and ZnFe2O4 to improve photocatalytic degradation of emerging organic pollutants, Ceramics International, 49 (2023) 4449-4459.

[18] V. Soni, Sonu, A. Sudhaik, P. Singh, S. Thakur, T. Ahamad, V.-H. Nguyen, L.-A.P. Thi, H.H.P. Quang, V. Chaudhary, P. Raizada, Visible-light-driven photodegradation of methylene blue and doxycycline hydrochloride by waste-based S-scheme heterojunction photocatalyst Bi5O7I/PCN/tea waste biochar, Chemosphere, 347 (2024) 140694.

[19] S.B. Prasanna, R. Sakthivel, K.C. Shanthakumar, S.A. Shivamurthy, Y.-C. Lin, U. Dhawan, X. Liu, R.-J. Chung, Dual Z-scheme Pr2Sn2O7/P@g-C3N4/SnS2 heterojunctions for the removal of tetracycline antibiotic by persulfate activation: Kinetics, thermodynamic parameters, density functional theory, and toxicity studies, Chemical Engineering Journal, 479 (2024) 147796.

[20] I. Idrees, A. Razzaq, M. Zafar, A. Umer, F. Mustafa, F. Rehman, W.Y. Kim, Silver (Ag) doped graphitic carbon nitride (g-C3N4) photocatalyst for enhanced degradation of Ciprofloxacin (CIP) under visible light irradiation, Arabian Journal of Chemistry, 17 (2024) 105615.

[21] N.Q. Thang, A. Sabbah, L.-C. Chen, K.-H. Chen, C.M. Thi, P. Van Viet, High-efficient photocatalytic degradation of commercial drugs for pharmaceutical wastewater treatment prospects: A case study of Ag/g-C3N4/ZnO nanocomposite materials, Chemosphere, 282 (2021) 130971.

[22] V.S. Manikandan, S. Harish, J. Archana, M. Navaneethan, Fabrication of novel hybrid Z-Scheme WO3@g-C3N4@MWCNT nanostructure for photocatalytic degradation of tetracycline and the evaluation of antimicrobial activity, Chemosphere, 287 (2022) 132050.